Vagal Nerve Complex in Normal Development and Sudden Infant Death Syndrome

L.E. Becker and W. Zhang

ABSTRACT: ***Background:*** Although the pathogenesis of sudden infant death syndrome (SIDS) is not understood, one of the major hypotheses is that a subtle defect in respiratory circuitry is an important underlying factor. The vagus nerve is a critical component of respiratory control, but its neuroanatomic complexity has limited its investigation in human disease. ***Methods:*** Correlating developmental studies on different parts of the vagus nerve allows a more comprehensive assessment of its maturation process. Comparison of the normal developing vagus nerve with nerves examined in SIDS patients suggests alterations in the nucleus tractus solitarius and dorsal vagal nucleus as well as in the peripheral vagus nerve. ***Results and Conclusions:*** The persistence of dendritic spines and lack of appropriate axonal growth implies delays in vagal maturation. Since nodose ganglia can be examined in vitro from autopsy material, perturbation to this system can be explored to evaluate further the mechanism involved in terminal vagal maturation. Although the reason for the delayed vagal maturation in SIDS is not apparent, the presence of astrogliosis in the region of the vagal nuclei is consistent with an exposure to hypoxic-ischemic events some time before death.

RÉSUMÉ: Complexe du nerf vague dans le développement normal et dans le syndrome de la mort subite du nourrisson. ***Introduction:*** Bien que la pathogenèse du syndrome de la mort subite du nourrisson (MSN) ne soit pas connue, une des hypothèses principales veut qu'un défaut subtil dans l'innervation du système respiratoire soit un facteur sous-jacent important. Le nerf vague est une composante critique du contrôle respiratoire. Cependant, sa complexité neuroanatomique en a limité l'investigation dans la pathologie humaine. ***Méthodes:*** La corrélation entre les études portant sur différentes parties du nerf vague permet une évaluation plus globale de son processus de maturation. La comparaison du nerf vague en développement et de nerfs de patients décédés du syndrome de la MSN suggère qu'il existe des altérations du noyau du faisceau solitaire, du noyau dorsal du vague ainsi que du nerf vague périphérique. ***Résultats et conclusions:*** La persistance d'épines dendritiques et l'insuffisance de la croissance axonale indiquent un retard de la maturation vaguale. Comme le ganglion inférieur du nerf vague provenant de matériel d'autopsie peut être examiné in vitro, une perturbation de ce système peut être explorée pour étudier le mécanisme impliqué dans la maturation du vague. Bien que la raison du retard de maturation du vague dans le syndrome de la MSN ne soit pas évidente, la présence d'astrogliose dans la région des noyaux du vague est compatible avec une exposition à des évènements hypoxiques-ischémiques avant le décès.

Can. J. Neurol. Sci. 1996; 23: 24-33

A major consideration in understanding the pathogenesis of sudden infant death syndrome (SIDS) is the presence of a subtle defect in the neural circuitry that controls respiration, particularly during sleep.[1] The vagus nerve is an important part of the respiratory control mechanism, carrying both afferent and efferent axons;[2] its complex includes the nucleus tractus solitarius (NTS), dorsal vagal nucleus (DVN), and nucleus ambiguus. The neuronal bodies of afferent fibers from the lungs and respiratory tract are located in the vagal nodose ganglia. Stretch and irritant receptors in the lungs and upper airway transmit information about the efficiency of gas exchange and the mechanics of ventilation to the NTS, the major sensory division of the vagal complex. Chemoreceptors in the carotid and aortic bodies relay information about pO_2, pCO_2 and pH to the NTS through the vagus and glossopharyngeal nerves. The NTS also receives input from the pontine and prepontine centers (amygdala, hypothalamus) in order to coordinate rate and depth of respiration with other motor and automatic behavior. Although poorly characterized anatomically, the neurons responsible for the rhythmic drive to breathing are located in the medulla and referred to as the central rhythm generator. Input from the NTS to the central rhythm generator determines the appropriate efferent

From the Department of Pathology, The Hospital for Sick Children, Toronto.
RECEIVED MARCH 8, 1995. ACCEPTED IN FINAL FORM AUGUST 28, 1995.
Reprint requests to: L.E. Becker, Department of Pathology, The Hospital for Sick Children, 555 Uniersity Avenue, Toronto, Ontario, Canada M5G 1X8

response to the motor neurons. These motor neurons are located in the dorsal respiratory group associated with the NTS and in the ventral respiratory group (nucleus retroambiguus and para ambiguus). Their descending synaptic connections are to the nucleus ambiguus innervating the pharynx and larynx, the phrenic nucleus innervating the diaphragm, and motor neurons innervating the intercostal muscles. Through the coordination of this respiratory control mechanism, the diaphragm contracts at the same time as the muscles of the upper airways relax, producing a smooth, coordinated mechanism for breathing. Critical to the efficiency of this mechanism is the integrity of the vagus nerve. The DVN is the major parasympathetic efferent system descending to and innervating the organs of the thorax and abdomen. Assessments of the components of the vagus nerve complex in normal development and in infants with SIDS have detected subtle differences in some of these anatomical regions.[3-13] The purpose of this review is to bring together, in the context of SIDS, the results of studies of these components, specifically, NTS, DVN, vagus nerve, and nodose ganglia.

Materials and Methods

From autopsies performed at The Hospital for Sick Children in Toronto, cases of SIDS were selected on the basis of standard criteria recently proposed by Willinger et al.:[14] "the sudden death of an infant under one year of age which remains unexplained after a thorough case investigation, including performance of a complete autopsy, examination of the death scene and review of the clinical history". All cases were investigated at the scene by police and the coroner's office. The number of cases varied from study to study. Control, non-SIDS cases were selected on the basis of a history of acute or sudden death, including children with congenital heart disease, acute infection, accidental asphyxia, acute trauma, and renal dysplasia. In none of these control cases was there evidence of significant neuropathology. In both SIDS and non-SIDS cases, the interval between death and autopsy was less than 24 hours. All ages have been expressed as postconceptional ages.

Brainstem (NTS, DVN)

A study of astrogliosis was conducted with 81 SIDS and 17 non-SIDS cases.[4] Brains were fixed in 10% neutral buffered formalin for a minimum of 10 days. The medulla was divided transversely into four blocks and embedded in paraffin. Serial sections from each block were cut at 7 μm, and 10-30 sections were taken from each block, yielding approximately 40-80 sections per case. Every tenth section was stained for astrocytes by the indirect immunoperoxidase method with antibody to glial fibrillary acidic protein (GFAP), according to established methods.[4] Astrocytes were counted if they displayed a GFAP-positive cytoplasm and counterstained nucleus. Cell counts were carried out with an ocular microscope and a cell counter at a magnification of 125X. The standard cross-sectional area of the DVN and the NTS was the target of cell counting in all cases. Since the nuclei were not regular geometric cylinders, their areas were different for each anatomic area. The cross-sectional areas of the DVN and NTS at all levels of the medulla were determined by an image-analyzing computer system (IBAS, Carl Zeiss, Germany). These areas were converted to templates on the microscope grid and the positive astrocytes within the template areas counted. All counts were unilateral.

The mean number of astrocytes was determined for each case in both DVN and NTS, and a rostral-to-caudal distribution was calculated by expressing the anatomic level of each stained transverse section as a percentage through the medulla. The medulla is about 3 cm long. Its rostral margin at the pons is distinct, but its caudal junction with the spinal cord is best identified as the upper rootlets of the first cervical nerve. Percentages through the medulla were determined with the aid of an atlas of the human brainstem.[15] Stained serial sections could be related to levels of the medulla by anatomical comparison by matching them with the plates in the atlas. The mean number of astrocytes for both groups of subjects was calculated at each level in the DVN and NTS. With the means and the cross-sectional area of the nuclei at each level known, the number of astrocytes per square mm was determined across each level in the DVN and NTS. A standard two-tailed Student *t*-test was used to determine the significance between the means of each group according to the level through the medulla.

For Golgi impregnation studies, 14 SIDS infants and 21 controls ranging in age from 20 weeks to 18 months were included.[10,13] Golgi staining was performed on fresh tissue that had been immediately immersed in Golgi fixative (osmium tetroxide 1 g, potassium diachromate 8 g, distilled water 300 ml), according to established methods.[10,13] Dendritic spine counts were performed in which the number of spines per 25 μm was calculated.[10,13] We examined 8-10 well-stained neurons. The areas of the medulla evaluated included the DVN and NTS. Developmental changes in spine density for each age group were evaluated at a distance of 20 to 260 μm from the soma of the neuron.

Vagus nerve

For this study, 30 cases of SIDS and 29 of non-SIDS were used and divided into 3 age groups: < 3 months, 3-6 months, and > 6-9 months.[3] In each subject, the left cervical vagus nerve proximal to the origin of the left recurrent laryngeal nerve was removed at autopsy. All the specimens were fixed by immersion in 3% gluteraldehyde in 0.1 m phosphate buffer (pH 7.4) for 12h at 4°C and postfixed in 2% osmium tetroxide in the same buffer for 1h. After dehydration through graded acetone (50-100%), each nerve was embedded in Epon with araldite, sliced into transverse sections (0.06-0.09 μm), and stained with uranyl acetate and then citrate.

Electron micrograph (EM) negative films were used for measurement. The grids were scanned under a Philips 201 electron microscope. One or two of the largest fascicles were chosen, and systematically selected areas were photographed from each specimen using 35mm EM film. The negatives, held as a film strip, were examined directly through a Tamron Photovix film video processor that projected a positive image onto a screen. The processor was coupled to an IBAS image analyzer (Zeiss Kontran, Carl Zeiss, Germany). Using previously established methods,[6] we determined axon size and frequency distribution for both myelinated and unmyelinated axon diameters. The fiber density, expressed as the number of myelinated and unmyelinated fibers per square mm, was calculated by using the total fiber number in the measured area. Myelin thickness, number of myelin lamellae, myelinated axon, and total fiber size were measured from electron micrographs at a magnification of 17,000X.

Nodose ganglia

In this study, pairs of nodose ganglia from 18 control and 5 SIDS infants were examined at autopsy. They were dissected free with 1 cm distal vagus nerve. One ganglia in each pair was fixed in 4% paraformaldehyde in 0.1 M phosphate buffer (pH 7.4) for 4-6 h. Tissue was oriented longitudinally, embedded in paraffin, cut at 6 μm, and stained with histologic and immunohistochemical preparations. The other ganglia from each pair was placed in a transport medium for cell culture, then further dissected with freeing of nerves and connective tissue. After being washed with alpha minimum essential medium (MEM), the ganglia were incubated for 2 hours at 37°C with 50 μmol dispase and 1,000 μmol per ml collagenase in alpha MEM. Mechanical trituration of these enzymatically softened ganglia was performed through a 5 ml plastic pipette. Cell clumps were then filtered using sterilized 37 mesh Nytex. Two ml of cell suspension were then layered on top of 6 ml of 25% isotonic percoll in the culture media (alpha MEM with 20% fetal bovine serum [FBS]). After incubation in the culture medium with 20% FBS for 24 h, cells were cultured in a medium with only 2% FBS. The cultured cells were fixed between days 4 and 7 with 4% paraformaldehyde for 20 min and washed with TRIS buffer for staining. For vagal body paraganglia (VBP) examination, the sections were cut at 10 μm and stained with hematoxylin and eosin (H & E). In sections where VBP were identified, the area was marked and tissue was embedded from the glass slide into Epon araldite, cut at 1 μm, and stained with toluidine blue. In sections in which VBP could still be identified, ultrathin sections were cut, stained with lead citrate uranyal acetate, and examined with an electron microscope. For each paraffin block, an average of 15 sections was cut at 6 μm and selectively stained with H & E and Bielschowsky stain. Indirect immunoperoxidase methods were used to examine both the VBP and nodose ganglia, using the following antisera according to established techniques: tyrosine hydroxylase (TH), chromogranin, synaptophysin, and antineurofilament. In four cases, high-pressure liquid chromotography (HPLC) was used for serotonin detection. Tissue was homogenized and extracted with 1 ml of perchloric acid containing 2.7 mM EDTA and 0.2 μmol 3,4-dihydroxy benzylamine. The extracts were filtered through 0.22 μm filters. The flow rate was 1 ml per min and the pressure 11.1 kPa. The absolute amount was calculated from peak 6, with reference to the serotonin standard (Sigma Chemical Co., St. Louis, MO).

Results

Brainstem (DVN, NTS)

This study[4] determined the distribution of reactive astrocytes throughout the rostro-caudal extent of the medulla. The areas examined for DVN ranged from 0.34 to 0.68 mm^2 and those for NTS from 0.39 to 1.54 mm^2. These represent the average area in square mm at each percentile throughout the medulla. The DVN was found to extend from the 10th to the 75th percentile and the NTS from the 5th to the 90th percentile of the total medullary length. The mean number of astrocytes per nuclear group and the number per square mm at each level of the medulla are shown in Figure 1. For DVN, the difference between SIDS and control infants reached its maximum at a distance of 45% to 65% through the medulla. Using the number of astrocytes per square mm, the study found the largest deviation in the same range. There were, however, differences at the 10th and 75th percentiles. Similar observations were evident in NTS, but the most significant differences were between the 45th and 90th percentiles. The polynomial regression lines calculated by computer showed that the SIDS group had a higher occurrence of gliosis than the controls. For DVN, the SIDS group differed significantly from controls in the average number of astrocytes per nucleus and the number of astrocytes per square mm. In NTS, the SIDS group differed significantly from controls in both the mean number of astrocytes and the mean number per square mm. The paired *t*-tests gave a level-by-level comparison of group means, the significance of which showed that the SIDS group had an increased level of gliosis along the length of both DVN and NTS.

Examination of the dendrites in the medulla in early gestation (20-24 weeks) showed that the somata of neurons were small and had short dendrites.[10] At later gestation (32-40 weeks),

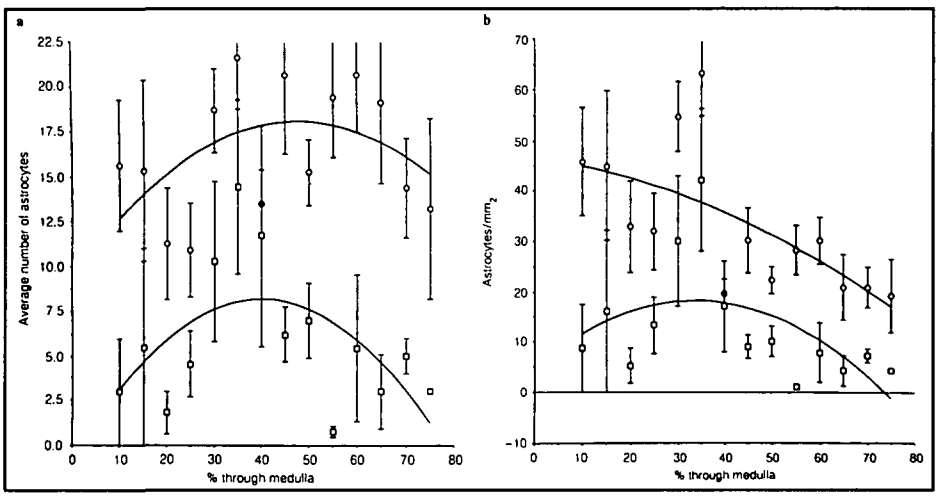

Figure 1: *From the NTS, mean number of astrocytes per nuclear group (A) and number of astrocytes per square mm (B) at each level of the medulla. The circles represent SIDS and the squares the controls.*

https://doi.org/10.1017/S0317167100039147 Published online by Cambridge University Press

dendrites gradually increased and spines appeared, particularly in the more distal regions. In infants older than 2 months, the somata of neurons were large and the dendrites were long with numerous branches. When spine density along the dendrite, 100-200 μm from the soma, was compared within each age group, the number of spines gradually increased with age from 20-36 weeks' gestation and then decreased rapidly. From 2-18 months of age, the spine density was low and did not change. In the SIDS victims, the distribution of dendritic spines showed a normal pattern: the number of spines decreased on the proximal dendrite and rose slightly distally, as was found in controls. Spine density was greater than that in controls in 12 of 14 cases examined. This difference in density between the 14 SIDS victims and the 7 controls aged 1 to 9 months was significant ($P < 0.01$). The density in the SIDS victims was similar to that of the term neonates (Figure 2); that is, the dendritic maturation was delayed in SIDS.

Vagus nerve

In normal maturation, significant growth of axons occurred between the groups < 3 months old and 3-6 months old. In SIDS, this growth did not occur; the size of myelinated vagal fibers (MVF) did not increase significantly between these two age groups. In infants < 3 months, no differences between controls and SIDS were noted. In infants between 3-6 months of age, significant differences were seen between SIDS and control subjects, with the diameter of MVF being less in SIDS.

When the percentage of MVF was assessed according to increasing diameter (Figure 3), the percentage of fibers less than 1 μm was found to be higher in SIDS patients than in controls. With fibers larger than 1 μm, the percentage was higher in controls. Therefore, there is a pronounced shift toward small MVF in these two age categories of SIDS. Because SIDS occurs uncommonly beyond 6 months, there were insufficient SIDS cases to compare with normal controls.

The diameter of unmyelinated vagal fibers (UVF) significantly increased between control groups < 3 and 3-6 months. The UVF diameters were significantly smaller ($P < 0.01$) in SIDS than controls in infants between 3 and 6 months of age (Table).

The density of MVF significantly increased between control groups aged < 3 and 3-6 months but not between the SIDS groups. There were no density changes of UVF between any of the control or SIDS groups. The total density of MVF and UVF per square mm did not change from one control or SIDS group to another.

The ratio of UVF to MVF was 6.78 in control group < 3 months but significantly lower, at 4.81 and 4.39, in control groups 3-6 and > 6-9 months, respectively. No differences between controls and SIDS were seen in any age category. There was no increase in the percentage of MVF in the total fascicle with increasing age in SIDS, whereas in control groups the percentage increased from 14% (< 3 months) to 17.5% (3-6 months) to 19.2% (> 6-9 months).

Linear regression analysis of axon diameter and myelin thickness revealed active myelination from the first to the second age group in both SIDS and controls, judged by a significant increase in the slope of the regressions. This finding was confirmed by a significant increase in myelin content, measured either as number of myelin lamellae or myelin thickness. No differences were apparent between SIDS and control infants.

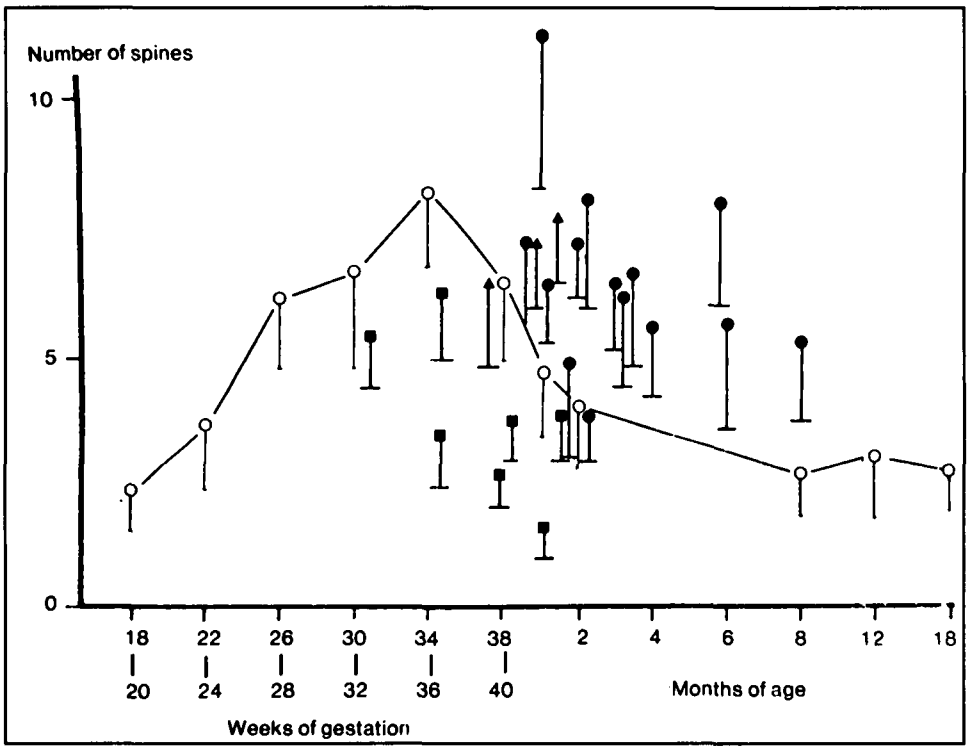

Figure 2: Developmental changes of dendrite spine density (number of spines per 25 μm) in the medullary reticular formation of SIDS (●), prematurely born SIDS infants (▲), ventilator-dependent prematurely born infants (■), and controls (O).

https://doi.org/10.1017/S0317167100039147 Published online by Cambridge University Press

Table: Comparison of myelinated and unmyelinated vagal nerve fibers in SIDS and control infants.[a]

Age	Size of MVF (nm)		Size of UVF (nm)		Density of MVF (per mm²)		Density of UVF (per mm)		Total density (per mm)		Ratio (UVF/MVF)	
	Control	SIDS	Control	SIDS	Control	SIDS	Control	SIDS	Control	SIDS	Control	SIDS
A <3 m (N = 10)	1493 ± 59[b] (N = 14)	1477 ± 273[b]	836 ± 62[b]	892 ± 76[b]	20702 ± 3103	21637 ± 4860	137815 ± 17499	122849 ± 20902	158517 ± 18418	144486 ± 23760	6.78 ± 1.28[c]	5.84 ± 1.14
B 3 <6 m (N = 10)	1637 ± 39[bd] (N = 14)	1466 ± 205	942 ± 86[c]	829 ± 72	26205 ± 4140	25552 ± 4167	123248 ± 23654	121600 ± 23654	149453 ± 25379	147152 ± 24880	4.81 ± 1.01	4.56 ± 0.73
C 6 <9 m (N = 9)	1784 ± 92[b] (N = 2)	1357 ± 182	932 ± 101	851 ± 20	25632 ± 5330	25706 ± 991	08104 ± 6668[d]	129981 ± 14429	133742 ± 10197	155687 ± 15420	4.39 ± 0.85	5.05 ± 0.38

[a]Values are expressed as means and standard deviations. SIDS indicates sudden infant death syndrome; MVF, myelinated vagal fibers; UVF, unmyelinated vagal fibers. Differences between SIDS and control subjects in each age group were calculated using Student *t*-test (two-tailed). Groups ABC (controls) and Groups AB (SIDS) had sufficient numbers for statistical analysis.

[b]Significantly different from next oldest age group of controls, $P < 0.01$.
[c]Significantly different from other two age groups of controls, $P < 0.01$.
[d]Significantly different between SIDS and control in the same age group, $P < 0.05$.
[e]Significantly different between SIDS and control in the same age group, $P < 0.01$.

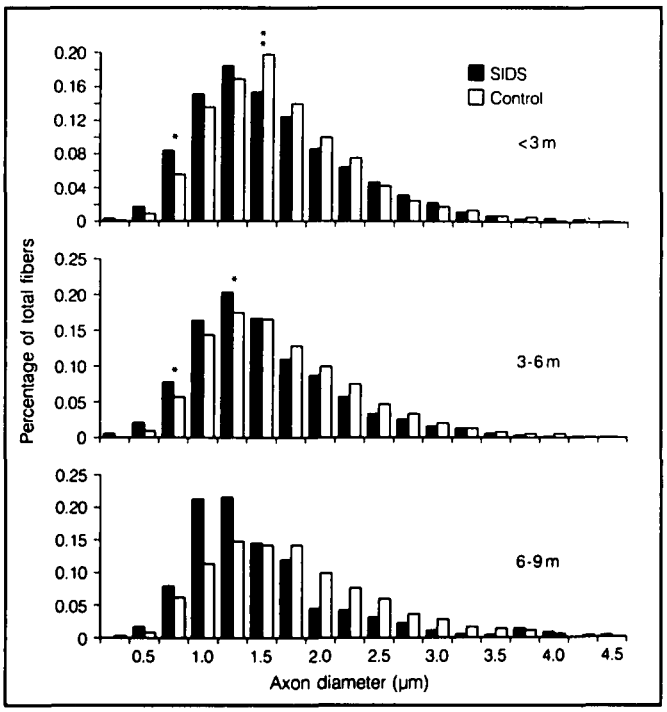

Figure 3: *Frequency distribution of cross-sectioned myelinated axonal diameters of the vagus nerve. Significant differences calculated for infants < 3 months old and those between 3 and 6 months are indicated as asterisked (P < 0.05), by Student t-test (two-tailed). No statistical analysis could be performed for infants between 6 and 9 months because the number of cases was insufficient.*

According to the ratio of axon diameter to total fiber diameter (G-ratio), three myelination conditions were identified in each group: hypermyelinated (< G < 0.6), optimally myelinated (0.6 < G < 0.7), and hypomyelinated (0.7 < G,1). The percentage of these conditions was compared between SIDS and control groups (Table). Significant differences in the percentage of optimally myelinated fibers was found through all age ranges; the percentage in controls ranged from 49.9 (< 3) to 52.7 (3-6) to 49.0 (> 6-9) in contrast to 35.2 (< 3) 40.4 (3-6), and 27.2 (< 6-9) in SIDS patients. The percentage of fibers with less myelin was greater in SIDS than controls but the differences did not reach statistical significance.

Nodose ganglia

Although small, VBP were identified as fusiform swellings on the vagus nerve in 72% of the specimens stained with H & E and Bielschowsky's stain. The number of discrete VBP identified in each section varied from one to four but was not related to age of infant. Anatomically, although VBP were frequently confined by the epineurial sheath and situated within the interstices of the vagus nerve, they appeared more often near the lower border of the nodose ganglia in association with prominent blood vessels. The average area on longitudinal section was 0.11 mm². Their size and shape varied slightly but no clear relationship to age was apparent. VBP were composed of single or, less frequently, multiple cellular lobules separated by a fine network of connective tissue and were surrounded by a thin layer of collagen fibers and fibrocytes. Chief cells were predominant and arranged in nests of varying size; sustentacular cells were more peripherally located. Chief cells had eccentric pyknotic nuclei and modest amounts of cytoplasm, while sustentacular cells had elongated nuclei with indistinct cytoplasm. Qualitatively, there were no differences between SIDS and control infants.

Ultrastructurally, chief cells in the VBP were characterized by relatively large, rounded nuclei with prominent nucleoli. In the cytoplasm, there were many membrane-bound osmiophilic dense granules (Figure 4A, B). The 100 cytoplasmic dense-core granules that were measured averaged 68 μm in diameter (mean 68.17 μm, SD 21.69, SE 2.16), varying from 26 to 124 μm, and were uniformly spherical. The number of granules was unevenly distributed among the cells. Endoplasmic reticulum was well developed. Mitochondria were swollen because of the post-mortem interval. Many spherical, homogeneous dense bodies of different sizes were also identified. In abutting chief cells, occasional paired membrane thickenings were present, resembling primitive forms of desmosomes (Figure 4C). Dark and light varieties of chief cells could not be readily distinguished.

The intervening processes of sustentacular cells separated individual cells or clusters of chief cells. The sustentacular nuclei had more consistent rims of chromatin than chief cells. Their cytoplasm was sparse, without granules, and nuclei were

https://doi.org/10.1017/S0317167100039147 Published online by Cambridge University Press

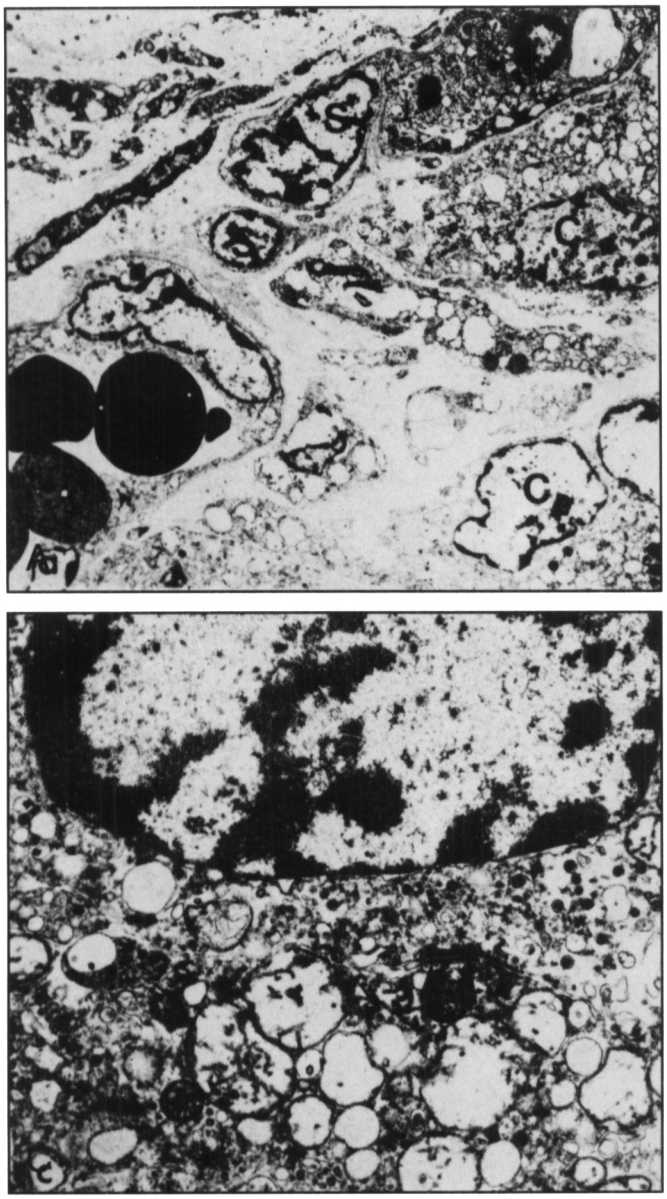

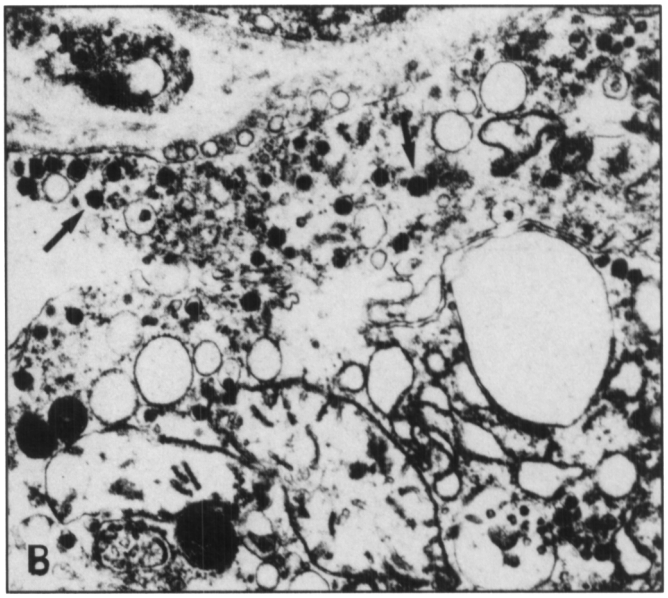

Figure 4: *(A) Vagal body paranganglia with chief cells (C) with cytoplasmic, membrane-bound osmiophilic dense granules, and sustentacular cells (S) with sparse agranular cytoplasm encircled by basal lamina. Electron micrograph, X 3400. (B) Chief cell with prominent neurosecretory granules (arrows). Electron micrograph, X 39,000. (C) Chief cell with cell junctions indicated by arrowheads. Electron micrograph, X 16,300.*

small. Basal lamina encircled these cells. There were about half as many sustentacular as chief cells. Interspersed between cells were fine nerve fibers, both myelinated and unmyelinated. Prominent fenestrated capillaries were also identified. Ultrastructurally, there were no differences between SIDS and control infants.

Immunohistochemical analysis of SIDS and controls indicated positivity with antiserum to serotonin in all VBP (Figure 5A-C) and no differences between the two groups. The chief cells were positive and the sustentacular cells non-reactive. Positive reaction with antiserum to chromogranin (Figure 5D), TH (Figure 5E), and synaptophysin (Figure 5F) was demonstrated in half of the VBP, again confined to chief cells. Sustentacular cells were reactive to antiserum against S-100 protein. HPLC confirmed the presence of serotonin in VBP.

In all cell cultures, following 12 h of seeding, dissociated large phase-bright cells were identified attached to the bottom of the glass well. At 3 days, some fine, distinct neurites were observed growing from them. In some cultures of 5-7 days, neuritic networks had become extensive. These phase-bright large cells, with or without neurites, were strongly stained with anti-neurofilament (NF) antibody (Figure 6). Remarkable case-to-case differences were observed in neuron population, neuron size, and length of neurite, excluding a meaningful comparison between the SIDS and control groups. The lowest number of NF immunoreactive neurons in one culture well was 22 and the highest 1315. The diameter of the smallest neuron was 8 μm and the largest 50 μm. The longest fiber of neuritic outgrowth was 1.46 mm. After 5-7 days, this culture system showed an increase of unhealthy-looking neurons, which were lightly stained with NF antibody and had an obscure nuclear profile. The cell cultures treated with Ara-C showed slightly decreased non-neuronal cells, more dead cells, and more clusters of aggregated neurons. At 7 days, the viability of cultured cells detected by trypan blue was 92% in one case and 94% in another.

In all the paraffin sections of nodose ganglia, approximately 30% or fewer of the neurons stained with TH antiserum compared with about 60% or more in the cell cultures. Figure 7A demonstrates TH-positive neurons with outgrowing neurites, which were dissociated from nodose ganglia at autopsy. Figure 7B shows TH-positive neurons in the section of nodose ganglia from the same specimen.

Discussion

The vagus nerve is composed of motor and sensory fibers and has a more extensive course and distribution than any other nerve. The three vagal nuclei in the brainstem include the DVN, NTS, and nucleus ambiguus. The rootlets of the

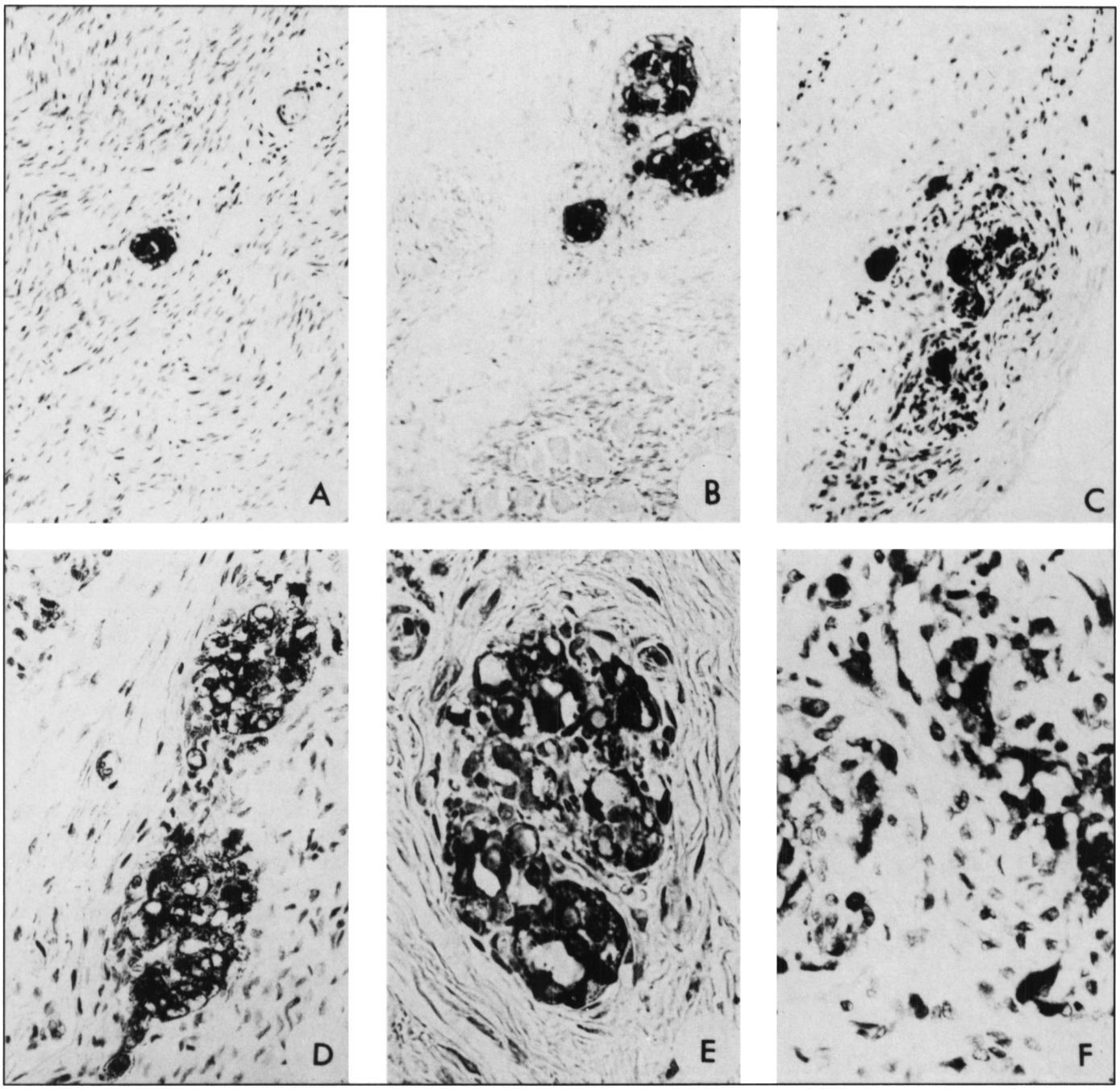

Figure 5: *Immunohistochemistry of vagal body paranganglia (VBP): (A) location of VBP within vagus nerve (anti-serotonin antiserum), X 100. (B) Location of VBP near the lower border of ganglia nodosum (anti-serotonin antiserum), X 100. (C) Location of VBP near the lateral edge of ganglia nodosum (anti-serotonin antiserum), X 100. (D) Positive reactive chief cells in VBP (anti-synaptophysin antiserum), X 400. (E) Positive reactive chief cells in VBP (anti-TH antiserum), X 400. (F) Positive reactive chief cells with VBP (anti-chromogranin antiserum), X 400.*

vagus unite into a single cord that leaves the cranium through the jugular foramen. Situated at this site are the superior ganglion, focused on general somatic sensibility, and the inferior ganglion (nodose ganglion), concerned with special visceral sensitivity from larynx, pharynx, lungs, and heart. The vagus nerve passes vertically down the neck, and the course of the right and left vagus differs as the nerves enter the thorax.

Because of its anatomic complexity, the vagus nerve has been difficult to evaluate developmentally[6,9] and pathologically.[3,8,16] Although some studies of an anatomic and physiologic nature have been carried out on experimental animals,[17-20] the data on the human vagus nerve are limited.

The key role that the vagus nerve plays in neural respiratory control has focused our interest on its development in infants in an effort to compare its characteristics to those of age-matched infants who die of SIDS. The first clue that this nerve could be abnormal in SIDS emerged from the observation that astrogliosis was present in the brainstem.[21] Our analysis of the location of

https://doi.org/10.1017/S0317167100039147 Published online by Cambridge University Press

Figure 6: *Dissociated vagal sensory neurons established in culture and confirmed by positive reaction with antisera to neurofilament. Immunoperoxidase, X 400.*

the astrogliosis identified, among many sites of involvement, the presence of reactive astrocytes in DVN and NTS.[12,22,23] These observations have been confirmed by others,[24-26] although not all studies have been able to show significant astrogliosis.[27] In our recent analysis,[4] we added to the cross-sectional assessment by evaluating the total rostral-caudal extent of DVN and NTS. We found significant astrogliosis, using the measurements of both reactive astrocytes per square mm and per nuclear area (DVN, NTS). Our results indicate that astrogliosis is significantly increased throughout the extent of these nuclei; however, they also show that the greatest difference between controls and SIDS is maximal at 50-75% though the medulla.

What does the astrogliosis imply? Although gliosis is not a specific reaction, it does suggest pathologic response to an insult. For example, repetitive hypoxic-ischemic episodes could "damage" the neuron in a fatal or non-fatal way. Astrogliosis would occur as a response to the injury.

Examination of the neurons of the DVN and NTS by conventional approaches shows no abnormality, but applying Golgi impregnation methods demonstrates subtle alterations in dendritic structure. Compared with age-matched controls, there were more dendritic spines in SIDS in our study.[10] In a similar study, Quattrochi et al.[7] found that spines persisted in 90% of SIDS but only 20% of control infants. Because of the developmental pattern of dendritic spine maturation (peaking at 34 to 36 weeks, then rapidly declining), the changes observed in SIDS suggest a delayed maturation with persistence of spines. It is postulated that the remodelling of dendrites is associated with more complex and mature neural function, possibly related to increasing maturation of respiratory control mechanisms.

Golgi impregnation defines dendritic ramifications but tells us little about the axonal component of the neurons of the DVN and NTS. Axons are best examined in the vagus nerve proper, where cross-sections allow a quantitative morphometric analysis not only of the axons but of their myelinating sheath. Our study[3] documents the difference between the growth of the vagus nerve in SIDS and control subjects during the first 9 months of life. The results show more small-diameter myelinated fibers in

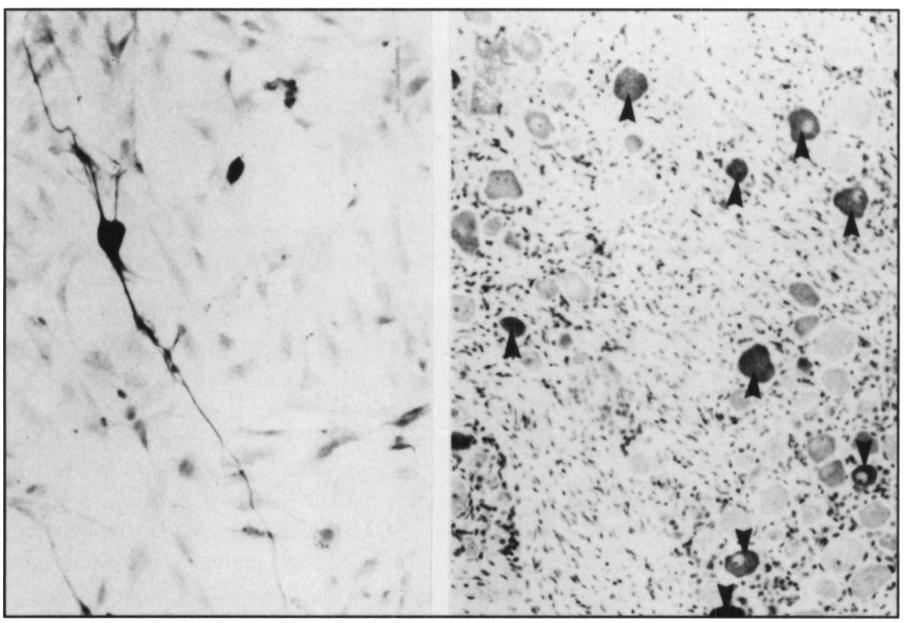

Figure 7: *(A) Vagal sensory neuron with neuritic extensions demonstrated by antisera to TH. Immunoperoxidase, X 400. (B) Positive reactive neurons (arrows) in nodose ganglia (anti-TH antiserum). Immunoperoxidase, X 100.*

SIDS, with inappropriately thin, hypomyelinated myelin sheaths. Linear regression analysis of myelin thickness and axon diameter found no significant differences between controls and SIDS. Similarly, the G ratios did not reveal a significant increase in hypomyelinated fibers in SIDS. Therefore, axonal growth appears to be delayed in the SIDS victims, reflected in the presence of more small-diameter fibers. This finding is supported by the data on the unmyelinated fibers, which showed significantly less axonal diameter in SIDS than controls between 3 and 6 months of age. The occurrence of delayed axonal growth in the vagus nerve and delayed dendritic maturation of neurons in the medulla suggest delayed neuronal maturation.

The vagus nerve contains afferent as well as efferent fibers. The neuronal soma of the afferent fibers is located in the superior and inferior vagal ganglia. The sensory neurons in the inferior or nodose ganglion are relevant to the lungs and upper respiratory tract.

The nodose ganglia have both neuronal and neuroendocrine components. To judge from animal studies, the cervical vagus nerve at the level of the ganglia is primarily an afferent nerve with fibers from abdominal and thoracic organs.[28] A small percentage are efferent fibers from the DVN, contributing to parasympathetic function. The ganglion cells are pseudounipolar with few synapses. Nevertheless, neurotransmitters and neuromodulators are synthesized and transported in neuronal cytoplasm and can be detected within these cells.[29] In animal studies, immunocytochemistry has demonstrated positivity for synaptophysin, calcitonin gene-related protein, substance P, neuron-specific enolase, and dopamine, but few human studies have been reported.[29-31] Determination of the developmental sequence in this ganglion is of special importance in infant disorders that suggest a delay in maturation such as SIDS.[1]

Our ability to culture neurons from autopsy tissue could allow some of the techniques learned from animal studies[32] to be applied to neurons derived from human tissue. In our culture system, neurites appear to be actively growing and developing bulb-like projections, suggesting that neurons dissociated from autopsy tissue retain the potential for viability and can recover and regenerate in limited ways. Dopaminergic neurons in these cultures were visualized using immunoperoxidase methods with TH antiserum. In most of the cultured neurons, TH-positive reactivity correlated with the positivity identified in paraffin sections of nodose ganglia. The higher proportion of TH-positive neurons in culture than in tissue may be due to the higher survival rate of these neurons, perhaps a result of their responsiveness to undefined neurotrophic factors in the culture medium. Viability of neurons in culture is affected by factors such as the interval between death and autopsy, cause of death, and course of the disease. Our results have demonstrated that dissociated vagal sensory neurons from autopsy tissue can survive at least 1 week when the interval between death and autopsy is less than 24 h. These neurons can be successfully cultured from autopsies of both infants and children. Neuronal cultures are difficult to set up because of the unpredictable frequency of tissue availability. If case and growth variables could be satisfactorily standardized, cultured vagal sensory neurons could prove to be a valuable model to study vagal developmental regulation, in SIDS compared to normal controls, independent of the complex vagal neural network that exists in vivo.

Paraganglia are widely distributed in the head and neck region, located in the middle ear, larynx, and vagus nerve. Embryologically, they are thought to arise from the neural crest, analogous to the chief cells of the carotid bodies. Although a chemoreceptor role has been experimentally established for carotid bodies, no distinct function has been assigned to the VBP.

Intravagal paraganglia have received scant attention, likely because of their small size. They have been described in an irregular distribution along the cervical, laryngeal, esophageal, and abdominal branches of the vagus nerve. The VBP are located just below the level of the nodose ganglia. Within the limited age range of cases examined, no relationship was found between age and number of VBP. It has been suggested[33] that VBP may have a local effect on vagal tone manifestations, which may include syncope, bradycardia, decreased ventricular contractility, and vasodepression. Hyperplasia of VBP has been noted in some patients with chronic hypoxemia.[5] Using qualitative assessment, we identified no hyperplasia in SIDS.

By histological analysis, the discrete lobular pattern resembles that of the carotid body. The most striking ultrastructural feature of the VBP is the abundance of cytoplasmic granules, also similar to that of carotid body. The remarkable structural resemblance suggests a functional similarity to carotid body.[34]

The immunoreactivity with antisera to chromogranin and synaptophysin correlates with the dense-core granules.[35] The presence of TH immunoreactivity indicates catacholamine within the VBP. Most important is the strong immunoreactivity with antisera to serotonin. The presence of serotonin is confirmed by HPLC.

Although the exact function of the VBP has not been determined, the presence of catacholamines and serotonin packaged in dense-core granules indicates that the chief cells play an active role in chemoreception. The location of VBP in intimate relationship to the vagus nerve and nodose ganglia suggests that the environment of this important neural relay station is being closely monitored. Presumably because of the strategic location of the nodose ganglia in the afferent pathway from all of the thoracic organs, monitoring by the VBP of alterations of pH, pCO_2, and pO_2 in this region could ensure appropriate corrective responses so that optimal conditions for neuronal functioning are maintained.

This review indicates the extent to which the normal development of the vagus nerve can be examined in human tissue. Although there are significant limitations to the interpretation of comparisons between "control autopsy" infants and SIDS victims, data from several centers indicate that changes are present in the vagus nerve complex. Delays in dendritic (DVN, NTS) and myelination (vagus nerve) maturation suggest that delayed maturation in SIDS may be a significant pathogenetic component. The relationship of delayed maturation to exposure to hypoxia-ischemia is undetermined, although the presence of astrogliosis in DVN and NTS would support this association. No abnormalities, however, were detected in nodose ganglia or vagal body paraganglia. Documentation of pathology in several parts of the vagus nerve also suggests the possibility of subtle dysfunction, which may have implications for interference with the complex developmental changes occurring in respiratory control during infancy and ultimately be a contributing factor to SIDS.

ACKNOWLEDGEMENTS

We would like to recognize the support of the Sudden Infant Death Syndrome Alliance and Canadian Foundation for the Study of Infant Deaths. This paper was prepared with the assistance of the Editorial Services, The Hospital for Sick Children, Toronto, Ontario, Canada.

REFERENCES

1. Becker LE. Neural maturational delay as a link in the chain of events leading to SIDS. Can J Neurol Sci 1990; 17: 361-371.
2. Feldman JL, McCrimmon DR, Smith JC, Ellenberger HH, Speck DF. Respiratory pattern generation in mammals. *In*: von Euler C, Langercrantz H, eds. Neurobiology of the Control of Breathing. New York: Raven Press, 1986: 157-164.
3. Becker LE, Zhang W, Pereyra PM. Delayed maturation of the vagus nerve in sudden infant death syndrome. Acta Neuropathol (Berl) 1993; 86: 617-622.
4. Bruce K, Becker LE. Quantitation of medullary astrogliosis in sudden infant death syndrome. Pediatr Neurosurg 1991-92; 17: 74-79.
5. Lack EE. Hyperplasia of vagal and carotid body paraganglia in patients with chronic hypoxemia. Am J Pathol 1978; 91: 497-516.
6. Pereyra PM, Zhang W, Schmidt M, Becker LE. Development of myelinated and unmyelinated fibers of human vagus nerve during the first year of life. J Neurol Sci 1992; 10: 107-113.
7. Quattrochi JJ, McBride PT, Yates AAJ. Brainstem immaturity in sudden infant death syndrome: a quantitative rapid Golgi study of dendritic spines in 95 infants. Brain Res 1985; 325: 39-48.
8. Sachis PN, Armstrong DL, Becker LE, Bryan AC. The vagus nerve and sudden infant death syndrome: a morphometric study. J Pediatr 1981; 98: 278-280.
9. Sachis PN, Armstrong DL, Becker LE, Bryan AC. Myelination of the human vagus nerve from 24 weeks postconceptional age to adolescence. J Neuropathol Exp Neurol 1982; 41: 466-472.
10. Takashima S, Becker LE. Developmental abnormalities of medullar "respiratory centres" in sudden infant death syndrome. Exp Neurol 1985; 90: 580-587.
11. Takashima S, Becker LE. Delayed dendritic development of chatecholaminergic neurons in the ventrolateral medulla of children who died of sudden infant death syndrome. Neuropediatrics 1991; 22: 97-99.
12. Takashima S, Armstrong D, Becker L, Bryan C. Cerebral hypoperfusion in the sudden infant death syndrome? Brainstem gliosis and vasculature. Ann Neurol 1978; 4: 257-262.
13. Takashima S, Mito T, Becker LE. Neuronal development in the medullary reticular formation in sudden infant death syndrome and premature infants. Neuropediatrics 1985; 16: 76-79.
14. Willinger M, James LS, Catz C. Defining the sudden infant death syndrome (SIDS). Deliberation of an expert panel convened by the National Institute of Child Health & Human Development. Pediatr Pathol 1991; 11: 677-684.
15. Olszewski J, Baxter D. Cytoarchitecture of the Human Brain Stem, 2nd ed. Basal: Karger, 1982.
16. Guo Y-P, McLeod JG, Baverstock J. Pathological changes in the vagus nerve in diabetes and chronic alcholism. J Neurol Neurosurg Psychiatry 1987; 50: 1449-1453.
17. Daly M de B, Evans DHL. Functional and histological changes in the vagus nerve of the cat after degenerative section at various levels. J Physiol 1953; 120: 579-595.
18. De Neef KJ, Jansen JR, Versprille A. Developmental morphology and physiology of rabbit vagus nerve. Brain Res 1982; 256: 265-274.
19. Schäfer K, Friede RL. The onset and rate of myelination in six peripheral and autonomic nerve of the rat. J Anat 1988; 159: 181-195.
20. Hasan SU, Sarnat HB, Auer RN. Vagal nerve maturation in the fetal lamb: an ultrastructural and morphometric study. Anat Rec 1993; 237: 527-537.
21. Naeye RL, Ladis D, Drage JS. Sudden infant death syndrome: a prospective study. Am J Dis Child 1976; 130: 1207-1210.
22. Becker LE. Neuropathological basis for respiratory dysfunction in sudden infant death syndrome. *In*: Tildon JT, Roeder LM, Steinschneider A, eds. Sudden Infant Death Syndrome. New York: Academic Press, 1983: 99-114.
23. Becker LE, Takashima S. Chronic hypoventilation and development of brainstem gliosis. Neuropediatrics 1985; 16: 19-23.
24. Ambler MW, Neave C, Sturner WQ. Sudden and unexpected death in infancy and childhood: neuropathologic findings. Am J Forensic Med Pathol 1981; 2: 23-30.
25. Kinney HC, Burger PC, Harrell FE Jr, Hudson RP Jr. 'Reactive gliosis' in the medullar oblongata of victims of the sudden infant death syndrome. Pediatrics 1983; 72: 181-187.
26. Summers CG, Parker JC Jr. The brain stem in sudden infant death syndrome: a postmortem survey. Am J Forensic Med Pathol 1981; 2: 121-127.
27. Pearson J, Brandeis L. Normal aspects of morphometry of brainstem astrocytes, carotid bodies, and ganglia in SIDS. *In*: Tildon JT, Roeder LM, Steinschneider A, eds. Sudden Infant Death Syndrome. New York: Academic Press, 1983: 115-122.
28. Mei N, Condamin M, Boyer A. The composition of the vagus nerve of the cat. Cell Tissue Res 1980; 209: 423-431.
29. Helke CJ, Hill KM. Immunohistochemical study of neuropeptides in vagal and glossopharyngeal afferent neurons in the rat. Neuroscience 1988; 26: 539-551.
30. Helke CJ, Niederer AJ. Studies in the coexistence of substance P with other putative transmitters in the nodose and petrosal ganglia. Synapse 1990; 5: 144-151.
31. MacLean DB, Bennett B, Morris M, Wheeler FB. Differential regulation of calcitonin gene-related peptide and substance P in cultured neonatal rat vagal sensory neurons. Brain Res 1989; 478: 349-355.
32. Katz DM, Erb M, Lillis R, Neet K. Trophic regulation of nodose ganglion cell development: evidence for an expanded role of nerve growth factor during embryogenesis in the rat. Exp Neurol 1976; 110: 1-10.
33. Lack EE. Microanatomy of vagal body paraganglia in infancy including victims of sudden infant death syndrome. Pediatr Pathol 1989; 9: 373-386.
34. Grimley PM, Glenner GG. Ultrastructure of the human carotid body. A perspective on the mode of chemoreception. Circulation 1968; 37: 648-665.
35. Gobbi H, Barbosa AJA, Teixeria VPA, Almeida HO. Immunocytochemical identification of neuroendocrine markers in human cardiac paraganglion-like structures. Histochemistry 1991; 95: 337-340.